A Corus Line: Nanophase Diagrams of Miscible Bimetallic Nanoparticles

Zhixuan Lin[1], E. Toulkeridou[2], Junlei Zhao[3], Yue Wang[1], Jeffrey E. Shield[4,5], and P. Grammatikopoulos[1,6,7*]

[1]Materials Science and Engineering, Guangdong Technion – Israel Institute of Technology, Shantou, Guangdong 515063, China

[2]Guangdong Technion – Israel Institute of Technology, Shantou, Guangdong 515063, China

[3]Department of Electronic and Electrical Engineering, Southern University of Science and Technology, Shenzhen 518055, China

[4]Mechanical and Materials Engineering, University of Nebraska-Lincoln, Lincoln, NE, 68588, USA

[5]Nebraska Center for Materials and Nanoscience, University of Nebraska-Lincoln, Lincoln, NE, 68588, USA

[6]Guangdong Provincial Key Laboratory of Materials and Technologies for Energy Conversion, Guangdong Technion – Israel Institute of Technology, Shantou, Guangdong 515063, China

[7]Instituto Regional de Investigación Científica Aplicada (IRICA) and Departamento de Física, Universidad de Castilla-La Mancha, 13071, Ciudad Real, Spain

E-mail: panagiotis.g@gtiit.edu.cn

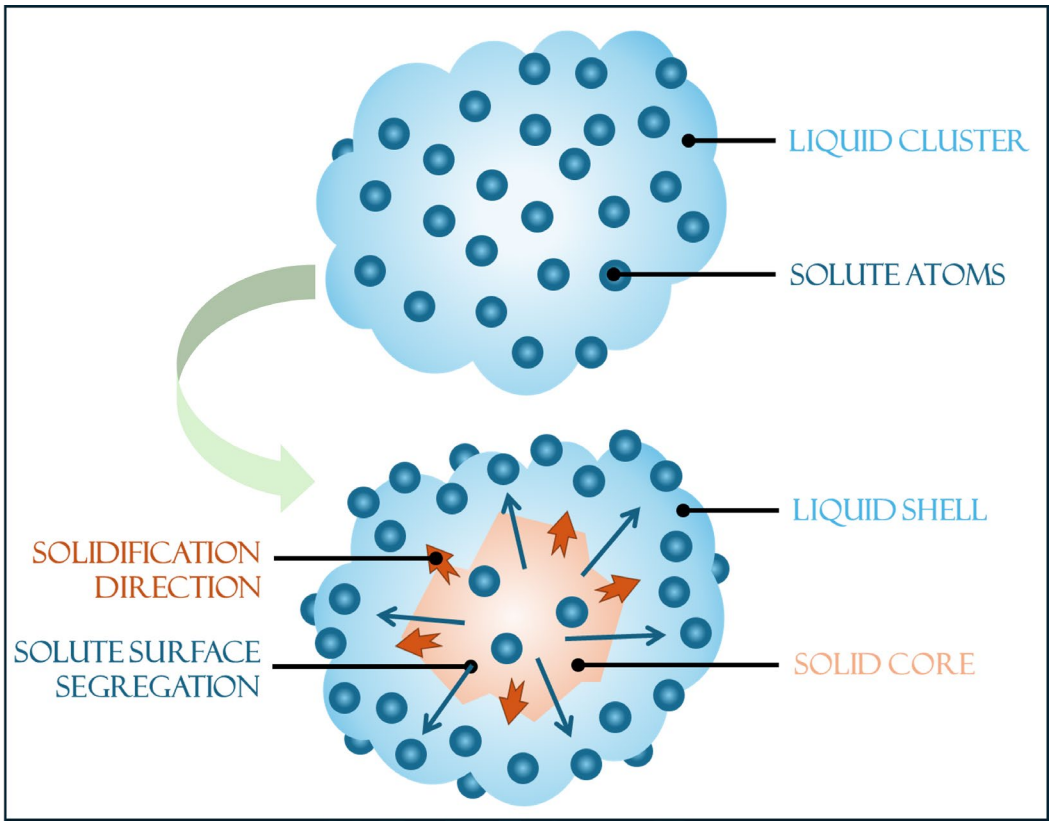

1. Regular solution model

To construct the phase diagram of nanoparticles (NPs), the regular solution model was employed to investigate their melting points. In an ideal solution, the assumption for the heat of mixing of its components is zero, and the entropy of mixing takes the same form as for ideal gases, where n is the total number of atoms, x_1 and x_2, corresponding to atoms of species A and B:

$$\Delta S_{\mathrm{mix}} = -nR(x_1 \ln x_1 + x_2 \ln x_2) \qquad (S1)$$

The regular solution model, originally introduced by Hildebrant and later generalised by Guggenheim, assumes negligible entropy change when a small quantity of a component is transferred from an ideal solution of similar composition, with the total volume remaining unchanged. This concept is explicitly stated by Guggenheim [S1]:

> "*A regular solution is one involving no entropy change when a small amount of one of its components is transferred to it from an ideal solution of the same composition, the total volume remaining unchanged*."

In this model, the entropy of mixing is treated as described in Eq. (S1), while acknowledging potential non-ideal behaviour. The focus of the regular solution model is on deviations of the enthalpy of mixing from its ideal values, which is a crucial aspect for solutions like metallic alloys. Several main assumptions are also made, including that (*i*) the interatomic interactions are pairwise; (*ii*) the coordination number z remains consistent across the solution and each of the pure components; (*iii*) interactions between atoms are limited to their z nearest neighbours; (*iv*) the interaction energy associated with a pair of atoms only depends on the type of atoms and not their concentration; (*v*) the occupancy of a site by an atom type is governed solely by the atom's concentration, without influence from neighbouring site occupancies [S2].

Utilising the regular solution model greatly simplifies the analysis of complex solutions, providing a dependable basis for computation. By bridging the gap between ideal and non-ideal solutions, the regular solution theory provides a framework for understanding and predicting the behaviour of systems that deviate from ideal solution assumptions [S1,S2]. However, this approach is not flawless due to its oversimplifying assumption and cannot perform well when the system is characterised by non-ideal mixing and complex atomic interactions. Besides, the model may predict a perfectly spherical structure where all atoms are precisely positioned in their ideal lattice sites, without any surface roughness or atomic-level deviations. Such perfect shapes are difficult to achieve by either experimental investigations or molecular dynamics (MD) simulations. Experimentally prepared NPs often exhibit surface defects, atomic-scale roughness, and may even be truncated or non-spherical. Similarly, in MD simulations, due to the complex

interactions and dynamical processes between atoms, the shapes of NPs can also deviate from their ideal geometric forms. Therefore, although the regular solution model provides a theoretical reference framework, one must be aware of the discrepancies between its predictions and reality.

2. Construction of nanophase diagrams

For the application of the regular solution model, the expressions for the solidus-liquidus line have been described by Guisbiers *et al.* [S3]. The method has been shown to work well for miscible systems [S4]:

$$\begin{aligned} RT\ln\left(\frac{x_{\text{solidus}}}{x_{\text{liquidus}}}\right) &= \Delta H_{\text{m}}^{\text{A}}\left(1-\frac{T}{T_{\text{m}}^{\text{A}}}\right)+\Omega_{\text{l}}\left(1-x_{\text{liquidus}}\right)^2-\Omega_{\text{s}}(1-x_{\text{solidus}})^2 \\ RT\ln\left(\frac{1-x_{\text{solidus}}}{1-x_{\text{liquidus}}}\right) &= \Delta H_{\text{m}}^{\text{B}}\left(1-\frac{T}{T_{\text{m}}^{\text{B}}}\right)+\Omega_{\text{l}}{x_{\text{liquidus}}}^2-\Omega_{\text{s}}{x_{\text{solidus}}}^2 \end{aligned} \tag{S2}$$

In Eq. (S2), $R = N_0 K_b$ is the ideal gas constant, x_{liquidus} and x_{solidus} are the compositions of liquid and solid phases at temperature T, Ω_{l} and Ω_{s} are the size-dependent interaction parameters/energy in the liquid and solid phases, T_{m}^{A} and T_{m}^{B} are the melting temperature of pure components A and B, $\Delta H_{\text{m}}^{\text{A}}$ and $\Delta H_{\text{m}}^{\text{B}}$ are the molar mixing enthalpies of A and B. Therefore, with specific T, x_{liquidus} and x_{solidus} values, $\Omega_{\text{l},\infty}$ and $\Omega_{\text{s},\infty}$ can then be determined. ($\Omega_{\text{l},\infty}$ and $\Omega_{\text{s},\infty}$ corresponding to the Ω_{l} and Ω_{s} at bulk situation.) This paper hereby firstly determined x_{liquidus} and x_{solidus} at $T \cong (T_{\text{m}}^{\text{A}} + T_{\text{m}}^{\text{B}})/2$ of their bulk phase diagram.

To transform bulk phase diagrams to nanoscale phase diagrams, all size-dependent parameters need to be reevaluated. A linear function of $1/D$, where D is the length edge of a polyhedral NP, is used:

$$\frac{\Phi}{\Phi_{\infty}} = 1 - \frac{\alpha_{\text{shape}}}{D} \tag{S3}$$

where Φ and Φ_{∞} are the nanoscale and bulk property parameters, respectively (namely, T_{m}^{A} and T_{m}^{B}, $\Delta H_{\text{m}}^{\text{A}}$ and $\Delta H_{\text{m}}^{\text{B}}$, $\Omega_{\text{l}}^{\text{A}}$and Ω_{s}^{B}). The shape-dependent parameter α_{shape}, which quantifies the size effect on the material property, is defined as:

$$\alpha_{\text{shape}} = \frac{AD(\gamma_{\text{s}} - \gamma_{\text{l}})}{V\Delta H_{\text{m},\infty}} \tag{S4}$$

where A/V is the surface area-to-volume ratio, $\Delta H_{\text{m},\infty}$ is the bulk melting enthalpy, and $\gamma_{\text{s(l)}}$ is the surface energy in the solid (liquid) state [S4]. The ratio between the number of surface atoms and the total number of atoms can be generalised as:

$$\frac{N_{\text{surf}}}{N_{\text{tot}}} = X_{\text{hkl}} a \frac{A}{V} \tag{S5}$$

where X_{hkl} is a numerical constant which only depends on the crystal orientation, and a is the bulk lattice parameter [S5]. Combining Eqs. (S3), (S4), and (S5) we get Eq. (S6):

$$\frac{\Phi}{\Phi_{\infty}} = 1 + \left(\frac{N_{\text{surf}}}{N_{\text{tot}}} \frac{1}{a X_{\text{hkl}}}\right)\left(\frac{\gamma_{\text{l}} - \gamma_{\text{s}}}{\Delta H_{\text{m},\infty}}\right) \Leftrightarrow \frac{\Phi}{\Phi_{\infty}} = 1 + \left(\frac{A}{V}\right)\left(\frac{\gamma_{\text{l}} - \gamma_{\text{s}}}{\Delta H_{\text{m},\infty}}\right) \tag{S6}$$

For every material and for different sizes [S4]:

$$\gamma_{\text{s}} = \frac{N_{\text{shape1}} A_{\text{shape1}} \gamma_{\text{shape1}} + N_{\text{shape2}} A_{\text{shape2}} \gamma_{\text{shape2}} + \cdots}{A} \tag{S7}$$

Using the surface area and volume equations specific to the shape of the NPs, the values of A and V can be geometrically derived. Consequently, all the parameters in Eq. (S5) are known, enabling the calculation of Φ. Substituting the calculated parameters, the size-dependent interaction $\Omega_{\text{s(l)}}$ can be determined, which enables derivation of the phase diagram for all nm-scale particles by multiplying the nanoscale with the bulk property parameter.

It should be noted that when the particle size shrinks below ~3 nm, the lattice constant and surface energy may display a weak size dependence, which may limit the accuracy of the calculation method, thus making the produced nanophase diagram less reliable. Furthermore, below 3 nm, the thermodynamic stability of the clusters may also decrease, making it difficult to reflect phase transition behaviour. Therefore, to ensure that the investigation is conducted within a relatively reliable size range, avoid errors introduced at smaller scales, and guarantee thermodynamic stability, we started our calculations from 3 nm, to obtain more reliable results.

Table S1: Material property values from the literature used for the calculations. We opted for a limited number of sources for consistency.

Material properties	Ni	Pt	Au	Pd
Crystal structure	fcc	fcc	fcc	fcc
$T_{\text{melt},\infty}$ (K)[S7]	1728.3	2041.5	1337.33	1828
density (g/cm^3)[S7]	8.9	21.4	19.3	12
atomic weight (g/mol)[S7]	195.084	58.693	196.967	106.42
$\gamma_{\text{s,111}}$ (J/m^2)[S8]	2.011	2.299	1.283	1.92
$\gamma_{\text{s,100}}$ (J/m^2)[S8]	2.426	2.734	1.627	2.326
$\gamma_{\text{s,110}}$ (J/m^{-2})[S8]	2.368	2.819	1.7	2.225
γ_{l} (J/m^2)[S7]	1.725	1.866	1.128	1.5
$\Delta H_{\text{melt},\infty}$ (J/mol-1)[S7]	17480	22175	12552	16736

Table S2: Calculated Φ values for truncated-octahedral NPs 3-10 nm in diameter

	T (K)		ΔH (J mol^{-1})		Ω_s (J mol^{-1})		Ω_i (J mol^{-1})		Φ/Φ_∞	
	Ni	Pt	Ni	Pt	Ni	Pt	Ni	Pt	Ni	Pt
Bulk	1728.3	1828	17480	22175	148913		157685		—	
3nm	1176.914	1050.330	11903.88	11420.13	101409.8	76690.2	107383.5	81207.78	0.681	0.515
4nm	1315.236	1162.608	13302.28	14103.3	113322.8	94708.67	119998.3	100287.7	0.761	0.636
5nm	1397.468	1446.798	14133.97	15715.28	120408	105533.7	127500.9	111750.4	0.809	0.709
6nm	1451.772	1383.796	14683.2	16786.48	125086.9	112727.1	132455.4	119367.5	0.84	0.757
7nm	1491.992	1616.713	15089.98	17560.92	128552.3	117927.8	136124.9	124874.5	0.863	0.792
8nm	1520.904	1495.304	15382.4	18139.15	131043.4	121810.8	138762.8	128986.3	0.88	0.818
10nm	1562.383	1561.112	15801.92	18937.45	134617.4	127171.7	142547.2	134663	0.904	0.854
	Au	Pd	Au	Pd	Au	Pd	Au	Pd	Au	Pd
Bulk	1337.33	1828	12552	16736	138714		148771		—	
3nm	774.3141	742.168	7267.608	6794.816	80315.41	56317.88	86138.41	60401.03	0.579	0.406
4nm	915.359	1013.253	8585.568	9271.744	94880.38	76847.56	101759.4	82419.13	0.684	0.554
5nm	1000.323	1175.404	9388.896	10761.25	103758.1	89193.1	111280.7	95659.75	0.748	0.643
6nm	1056.016	1284.835	9916.08	11765.41	109584.1	97515.94	117529.1	104586	0.790	0.703
7nm	1096.611	1361.86	10292.64	12468.32	113745.5	103341.9	121992.2	110834.4	0.82	0.745
8nm	1126.344	1420.626	10568.78	13003.87	116797.2	107780.8	125265.2	115595.1	0.842	0.777
10nm	1168.826	1502.616	10970.45	13756.99	121236	114022.9	130025.9	122289.8	0.874	0.822
	Pd	Pt	Pd	Pt	Pd	Pt	Pd	Pt	Pd	Pt
Bulk	1828	2041.5	16736	22175	33897		34347		—	
3nm	742.168	1051.373	6794.816	11420.13	13762.18	17456.96	13944.88	17688.71	0.406	0.515
4nm	1013.253	1297.993	9271.744	14103.3	18778.94	21558.49	19028.24	21844.69	0.554	0.636
5nm	1175.404	1447.424	10761.25	15722.08	21795.77	24032.97	22085.12	24352.02	0.643	0.709
6nm	1284.835	1545.829	11765.41	16786.48	23829.59	25660.03	24145.94	26000.68	0.703	0.757
7nm	1361.86	1616.868	12468.32	17562.6	25253.27	26846.42	25588.52	27202.82	0.745	0.792
8nm	1420.626	1669.746	13003.87	18139.15	26337.97	27727.75	26687.62	28095.85	0.777	0.818
10nm	1502.616	1743.441	13756.99	18937.45	27863.33	28948.04	28233.23	29332.34	0.822	0.854

3. Results and Discussion

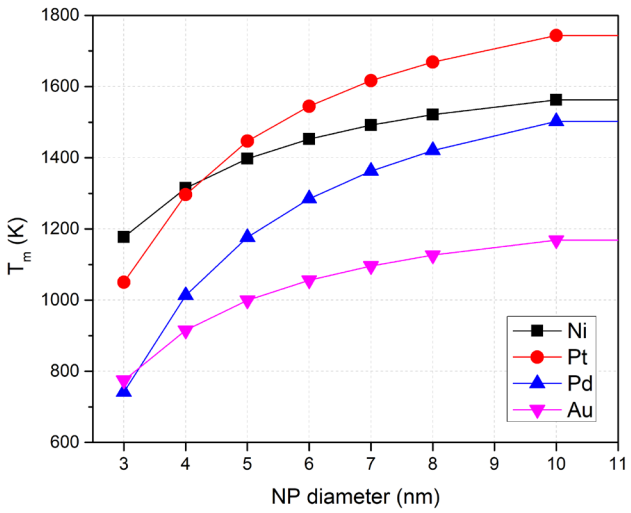

Figure S1: Melting points as a function of NP diameter for all monometallic systems studied here, indicating the different rates of melting point depression among different elements.

Movie S1: MD study of coalescence between monometallic Pd and Pt NPs at 1200 K. The temperature is below the NPs' melting points. Amorphous, partially segregated NPs emerged, with a tendency of Pd atoms to occupy surface sites.

Movie S2: MD study of coalescence between monometallic Pd and Pt NPs at 1600 K. The temperature is above the NPs' melting points. Liquid, mixed NPs emerged, which, upon cooling, may result in cored, partially demixed NPs.

References

S1. J. Hildebrand, The term 'regular solution', *Nature* 168, 868 **(1951)**. https://doi.org/10.1038/168868a0

S2. B.S. Bokstein, M.I. Mendelev, D.J. Srolovitz, *Thermodynamics and kinetics in materials science: a short course*, Oxford University Press, Oxford, UK **(2005)**. ISBN 0 19 852803 5 (Hbk) 978-0-19-852803-6
ISBN 0 19 852804 3 (Pbk) 978-0-19-852804-3

S3. G. Guisbiers, S. Mejia-Rosales, S. Khanal, F. Ruiz-Zepeda, R.L. Whetten, M. José-Yacaman, Gold-copper nanoalloy, "Tumbaga", in the era of nano: phase diagram and segregation, *Nano Lett* 14, 6718 **(2014)**. https://doi.org/10.1021/nl503584q

S4. G. Guisbiers, G. Abudukelimu, Influence of nanomorphology on the melting and catalytic properties of convex polyhedral nanoparticles, *J Nanopart Res* 15, 1431 **(2013)**. https://doi.org/10.1007/s11051-013-1431-x

S5. J.D. Honeycutt, H.C. Andersen, Molecular dynamics study of melting and freezing of small Lennard-Jones clusters, *J Phys Chem* 91:19, 4950–4963 **(1987)**. https://doi.org/10.1021/j100303a014

S6. G. Guisbiers, S. Khanal, F. Ruiz-Zepeda, J. Roque de la Puente, M. José-Yacaman, Cu-Ni nano-alloy: mixed, core-shell or Janus nano-particle?, *Nanoscale* 6, 14630 **(2014)**. https://doi.org/10.1039/C4NR05739B

S7. *Springer Handbook of Condensed Matter and Materials Data*, W. Martienssen and H. Warlimont eds. Springer, Heidelberg, **(2005)** p.124, 125, 60, 61. https://doi.org/10.1007/3-540-30437-1

S8. L. Vitos, A.V. Ruban, H.L. Skriver, J. Kollár, The surface energy of metals, *Surf Sci*, 411:1–2, 186 **(1998)**. https://doi.org/10.1016/S0039-6028(98)00363-X